# Segmentation of Multiple Sclerosis Lesions using Quantitative MRI

**D. R. Lang[1], V. Ermer[1], N. J. Shah[1,2], and H. Neeb[3]**

[1]Institute of Neurosciences and Biophysics, Research Centre Juelich, Juelich, Germany, [2]Faculty of Medicine, Department of Neurology, RWTH Aachen University, JARA, Aachen, Germany, [3]RheinAhrCampus Remagen, University of Applied Sciences Koblenz, Remagen, Germany

**Introduction:**

A fast and reliable method to quantitatively measure the absolute water content of the human brain *in vivo* has been recently developed [1,2,3]. Simultaneously, parameter maps of $T_1$ and $T_2$* can be acquired. These quantitative parameter maps are very sensitive for the detection of subtle pathological changes in a variety of neurological diseases, such as multiple sclerosis (MS). During the course of MS, the myelin sheet which surrounds nerve fibres is destroyed. In these regions, inflammation is prominent resulting in an approximately 8 % higher water content than observed for healthy white matter (WM). In particular, the implementation of automated segmentation of WM lesions in MS patients might offer the possibility to accurately segment datasets from a large number of patients. Importantly, the precision of the segmentation is not observer dependent. The segmentation of abnormal regions in the brain, such as MS lesions, has recently gained attention [4,5], but quantitative MR images were not the basis. Using quantitative MRI, national and international multi-centre studies can be directly compared and, in addition, longitudinal studies for sensitive disease monitoring can be more easily realised. Finally, quantitative imaging might potentially provide additional disease markers for an improved diagnosis and accurate stage monitoring of the disease.

**Methods:**

To quantitatively measure the absolute water content in the brain, a fast and reliable method developed recently was used [3]. Based on an acquired series of spoiled gradient echo images with different $T_2^*$-weighting (*QUTE*) [1,2], the water content, $T_1$ and $T_2^*$ were simultaneously mapped. Furthermore, FLAIR images were acquired as they are a well-established 'gold standard' for MS diagnosis and can be directly compared to the segmentation results. As a first step, the $T_1$ maps were segmented into WM, grey matter (GM) and cerebrospinal fluid (CSF) using a univariate histogram-based approach. Based on the reconstructed $T_1$ maps [1], $T_1$ values in the range of [450, 800] ms are assigned to WM, values in the range of (800, 1500] ms to GM and values in the range of (1500, $\infty$) ms to CSF. In order to improve this univariate approach, the additional information contained in the water content maps was also used. As water content and $T_1$ are correlated, the 2D (water content, $T_1$) averages for the WM and GM segment resulting for the univariate approach were calculated. Then, water content and $T_1$ values were projected onto the connecting line between the WM and the GM average in the 2D distribution of water content vs. $T_1$. The resulting histogram was fitted with a polynomial function of 5$^{th}$ degree in order to determine the minimum between the WM and GM peak. This minimum is used as an intersection to calculate an orthogonal to the connecting line of the 2D averages, which can then be used as a separation criterion for the segmentation of WM and GM. Using this preliminary information of the different tissue types, lesions in WM can now be identified and further characterised. Therefore, the difference between the water content maps of MS patients and a quantitative water content brain atlas, consisting of 35 young and healthy volunteers [6], was calculated for the WM segment. Thus, the water content maps of the MS patients were first normalised and co-registered (SPM5 [Wellcome Department of Cognitive Neurology, www.fil.ion.ucl.ac.uk]) to the quantitative water content atlas. In the resulting difference image between MS watermap and atlas, values greater than the 95 % quartile are defined as lesions. To minimise false positive classifications, only lesions which were also identified in the slices above and below and which showed a roundness > 0.7 were stored in the lesion mask. Based on the multivariate segmentation with different predefined thresholds for CSF, a second lesion segmentation approach based on lesion characteristics such as $T_1$ relaxation time was developed in order to segment lesions which were missed by the atlas based segmentation. Using two different thresholds for CSF (1500 ms and 2500 ms) during the multivariate segmentation, lesions were identified by a connected component search in the GM segment. The GM segment was used as the water content and $T_1$ distributions of MS lesions typically overlap with those in GM. Using different CSF thresholds enables a more sensitive detection especially of lesions with higher $T_1$ and water content, as the resulting GM segment is partly determined by the initial separation of CSF. In order to minimise the number of falsely positive classified lesions, the size and circularity of lesions as well reference lesion voxels (described above) were incorporated in the segmentation process as additional information. In combination with the lesion mask resulting from the atlas segmentation, a final lesion mask was created.

**Results:**

In this study, 8 patients were used for the evaluation of the proposed methods. The results of the univariate (a) und multivariate tissue segmentation (b) are shown in Figure 1. The multivariate approach shows a lower number of GM voxels predominantly located in deep WM. The corresponding histograms of the $T_1$ distributions for both approaches are presented in Figure 2. The vertical blue lines represent the threshold between WM and GM and GM and CSF, respectively, which were used for univariate segmentation. Both distributions are almost identical except the transition between WM and GM (blue region) resulting from the univariate approach. The WM segments based on the multivariate segmentation are approximately 19.67 % larger and the GM segments are about 11.16 % smaller than those of the univariate segmentation. In Figure 3, one representative slice of the final lesion segmentation is shown. The tissue image (a) after lesion segmentation and the corresponding FLAIR image (b) are presented. All existing lesions were visually counted in the FLAIR images and compared to the results of the segmentation. In total, 64.57 % of the lesions were classified as true positive and 35.43 % were not detected. In total, 77.42 % of all segmented lesions were exactly segmented and 22.58 % of lesion were classified as false negative.

**Discussion:**

The lesion segmentation algorithm provides very stable results, especially with respect to the relatively low rate of false positive detected lesions. This segmentation provides the basis for the implementation of supervised learning algorithms. Implementing a non-linear learning algorithm, such as support-vector-machines using a polynomial kernel or a k-nearest neighbour approach might provide even better results, especially with respect to the relatively high false negative rate observed. The latter can be attributed to the very stringent criteria imposed in order to minimise the false positive rate which is a pre-requisite for any supervised learning approach where the lesions detected for the required training sample. However, using quantitative data as a basis for lesion segmentation might provide much more stable, possibly even unified, segmentation criteria. Those criteria are inherently more objective as they are smaller extend influenced by subject variability and completely independent on the scanner hardware or other environmental influences.

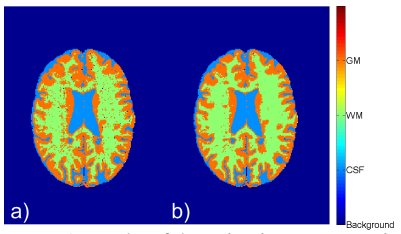


**Figure 1** a) Results of the univariate segmentation and b) of the multivariate segmentation

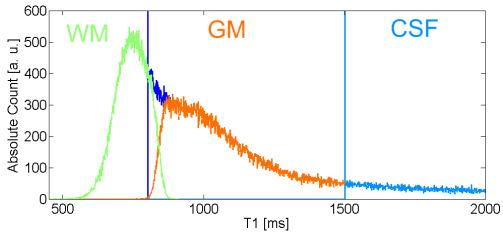


**Figure 2** Histograms of the $T_1$ distribution of the univariate and multivariate segmentation as presented in Figure 1.

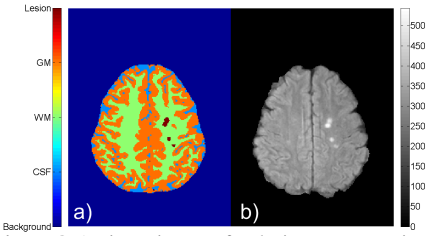


**Figure 3** a) Tissue image after lesion segmentation and b) corresponding FLAIR image.

**References:** [1] Neeb et al. NeuroImage 2006, 29(3):910-22, [2] Neeb et al. NeuroImage 2006, 31(3):1156-68, [3] Neeb et al. NeuroImage 2008, 42(3):1094-109, [4] Songyang et al. IEEE Int. Symp.on Biomed. Imaging 2002, [5] Wu et al. NeuroImage 2006, 32(3):1205-1215, [6] Ermer et al. Proceedings ESMRMB 2008, Epos #494